Electronic Supplementary Material (ESI) for Soft Matter.

Supplementary Material: Using Tobacco Mosaic Virus to Probe Enhanced Surface Diffusion of Molecular Glasses

Yue Zhang,[1] Richard Potter,[1] William Zhang,[1] and Zahra Fakhraai[1]

[1]*Department of Chemistry, University of Pennsylvania,*
Philadelphia, Pennsylvania 19104-6323, USA

(Dated: August 25, 2016)

EXPERIMENTAL DETAILS AND ADDITIONAL DISCUSSIONS

Material and film preparation

N,N$'$-Bis(3-methylphenyl)-N,N$'$-diphenylbenzidine (TPD, structure in figure S1) was purchased from Sigma-Aldrich and used without further purification, moelcular structure shown in S1. 400 nm films were prepared by physical vapor deposition (PVD) at a substrate temperature of bulk T_g (T_g = 330 K) with an average deposition rate of 0.2 nm/s. Details of the custom vacuum setup and procedures are published in our earlier work[1, 2]. Films were further annealed at T_g + 10 K (340 K) in vacuum oven overnight to anneal any stability or surface roughness. An AFM image of the surface of a typical sample is shown in Figure S2 that shows an initially flat morphology. The surface roughness is measured to be 0.91 nm.

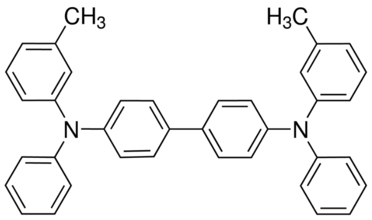

FIG. S1. Molecular structure of N,N$'$-Bis(3-methylphenyl)-N,N$'$-diphenylbenzidine (TPD).

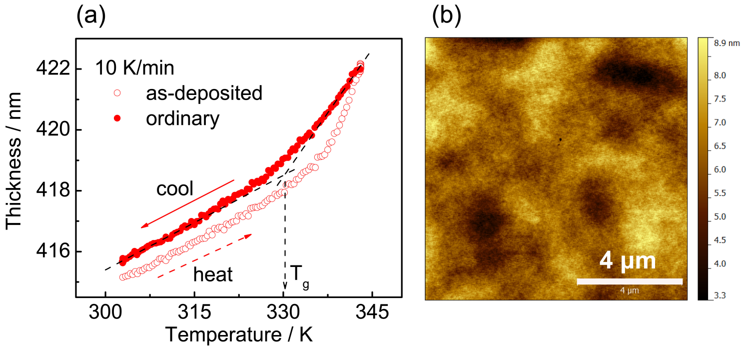

FIG. S2. (a) As-deposited 400nm TPD films were heated well above its bulk T_g to anneal away any stability and transform into ordinary liquid cooled glass. Film thickness as measured by ellipsometry during heating and cooling at 10 K/min. (b) Initial morphology of 400 nm TPD films after annealing at T_g+10 K in vacuum overnight. The surface roughness is measured to be 0.91 nm from AFM topography image.

Bulk Viscosity Measurement of Bulk TPD

Measurements of viscosity were performed on bulk TPD between 358 K and 373 K using rheometer (Bohlin CVO, Malvern Instruments). The data is shown in Fig. S3.

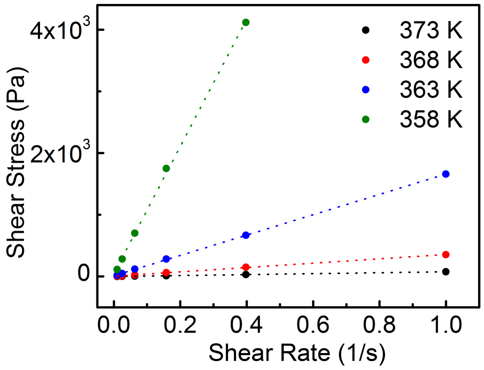

FIG. S3. Shear stress versus shear rate applied to bulk TPD at various temperatures ranging from 358 K to 373 K. Bulk viscosity was evaluated based on the slope of these curves.

TMV purification and deposition onto TPD films

Dried leaves infected by tobacco mosaic virus were purchased from ATCC (PV-598). Infected, dried leaves were pulverized into a grainy powder and was mixed with 3 mL of 0.2% -mercaptoethanol (Sigma-Aldrich) and 3 mL of 0.01 M phosphate buffer (pH 7.8) (Sigma-Aldrich). This solution was centrifuged for 15 minutes at 9,000 rpm and the resulting supernatant was saved, to which 80 L of 1-butanol (8 mL/100 mL extract) (Sigma-Aldrich) were added to coagulate chloroplasts and centrifuged again for 30 minutes at 9,700 rpm. The resulting aqueous supernatant was saved and dialyzed in miliQ water using mini-dialysis devices (ThermoFisher Scientific, Slide-A-Lyzer$^{\text{TM}}$ MINI Dialysis Device, 20K MWCO, 0.1 mL). 100 L of the dialyzed TMV solution was pipetted onto the annealed TPD films, spin-coated for 3 minutes at 500 rpm and dried with nitrogen for further isothermal imaging measurements. On Si substrate, the height of TMV is measured to be 16.6 ± 0.2 nm with AFM. The process of spin-coating of TMV on TPD surface does not alter the surface morphology or the properties of the TPD film.

Isothermal annealing and AFM imaging procedure

Isothermal annealing experiments were performed using a custom thermoelectric heating-stage, equipped with a thermoelectric module (Custom Thermoelectric TEC) and a thermistor (Oven industries TR91-170) to measure the value of the temperature, along with a DC power supply to control the temperature (Mastech HY3010E). The temperature of the heating-stage was calibrated with melting-point standards ($C_{13}H_{10}O$) $T_m = 48.0 \pm 0.3$ °C and ($C_{18}H_{36}O_2$) $T_m = 69.6 \pm 0.3$ °C (Sigma-Aldrich), the temperature fluctuations were within ± 2 K throughout the experiments in the temperature range used in this study. After identifying an isolated TMV particle, the sample temperature was brought to desired annealing temperature (stabilize within a minute), the surface was then continuously imaged using non-contact atomic force microscopy (AFM, Agilent 5420). Non-contact AFM tips (Budget Sensors, Tap-300G, resonance frequency 300 kHz, tip radius of curvature <10 nm, force constant 40 N/m) were used for these measurements.

Extracting line profiles from AFM images

Here we show an example of how we extract line profiles from AFM topography images. Due to the large aspect ratio of TMV virus, enough statistics can be obtained from multiple line profiles near the center of the nanorod, resulting in very reproducible profiles. In top figure of S4, line 1 and line 3 defines the range of 2D flow without the effect from the two end regions of TMV. In the bottom panel, we show the line profiles from lines 1, 2 & 3, they overlap perfectly indicating the validity of 2D flow assumption across the virus.

Wettibility of TPD on TMV

To demonstrate that TPD can completely wet the TMV virus, in S5 we show the spontaneous wetting and embedding of TMV on a bulk TPD film at an annealing temperature of 323 K (T_g - 7 K). The images shown in Figure S6 demonstrate that TPD can quickly and completely wet the TMV virus, reaching a zero final contact angle. As such, even at lower temperatures the zero contact angle implies that the virus is completely wet with a layer of TMV and the meniscus evolution after some transient time is independent of the contact

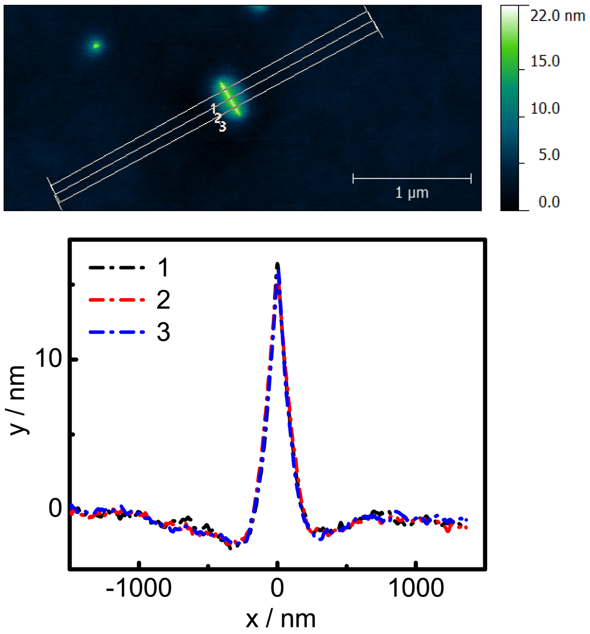

FIG. S4. Typical line profiles obtained from AFM topography image. Top: AFM topography of a single TMV nanorod on TPD glass surface, line profiles were obtained from perpendicular lines across the TMV. From top to bottom: line 1, line 2 and line 3. Bottom: The three line profiles obtained from the top image, the profiles perfectly overlap within instrument noise, indicating the validity of two dimensional flow assumption.

angle, or interactions of TPD with TMV.

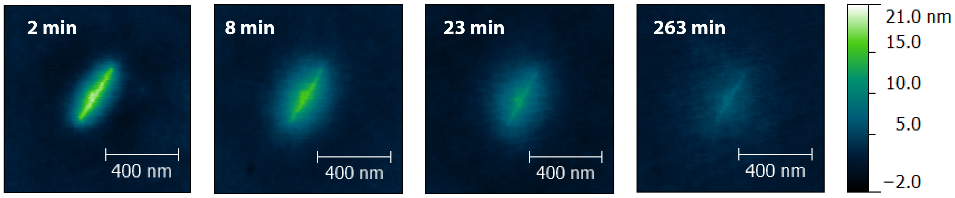

FIG. S5. AFM images of rapid wetting and embedding of TMV on bulk TPD surface at the annealing temperature of 323 K.

Additional profiles at all annealing temperatures studied

All the temporal profiles at five annealing temperatures surveyed in this study are shown in the left panel of S6. On the right panel, we show the self-similarity of the surface diffusion controlled process.

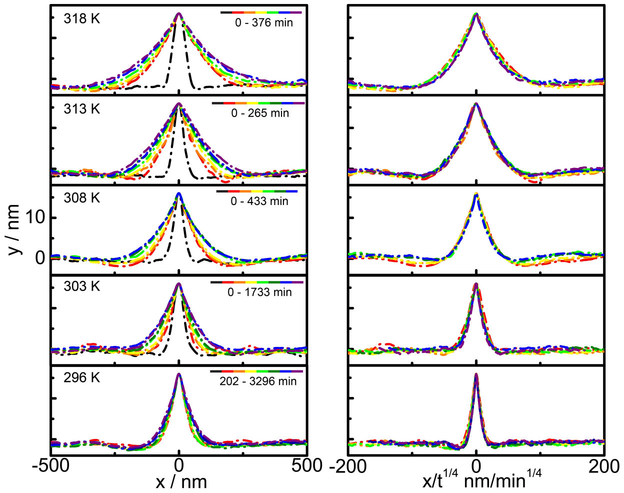

FIG. S6. Temporal profile evolution at various annealing temperatures and self-similarity of surface diffusion controlled evolution. Left panel: time evolution of the profiles across TMV at five different annealing temperatures, from top to bottom: 318 K (T_g - 12 K), 313 K (T_g - 17 K), 308 K (T_g - 22 K), 303 K (T_g - 27 K), 296 K (T_g - 34 K); Right panel: scaled profiles with respect to $t^{1/4}$ collapse onto the same curve, indicative of self-similarity nature of the surface diffusion control process.

Experimental data fit to numerical solution

Since TPD completely wets the virus, it is reasonable to assume that the profile shape after some initial transient time is independent of the surface energy of the virus. However, the height of the profile remains constant, indicating that there is little accumulation of material on top of the virus. This is not surprising as there is little driving force directly on top of the virus for diffusion. As such, one can assume that the solution for this problem is mathematically identical to having a step function with a constant hight towards which the molecules are attracted. Equation 1 has been solved for a constant step height boundary conditions [3–5]. Furthermore, in another work Benzaquen *et al.* numerically demonstrated that equation 1 would eventually evolve into the same universal curve even under a slightly different initial boundary condition[3]. The universal scaled profile can be written as $U = \frac{x}{t^{1/4}}(\frac{kT}{D_s\gamma\Omega^2\nu})^{1/4}$, where U is a scaled function of x and t. The experimental profiles were fit to the universal solution with a single fitting parameter $\frac{D_s\gamma\Omega^2\nu}{kT}$, where surface diffusion coefficient D_s can be evaluated.

TMV height versus time at annealing temperatures studied

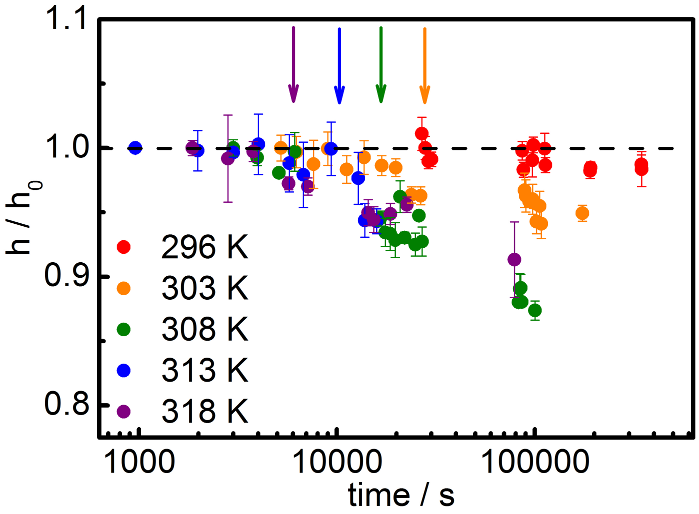

FIG. S7. Normalized apparent height of the TMV virus versus annealing time at various annealing temperatures. Dashed line shows the TMV height before embedding and colored arrows show the time at which embedding becomes apparent beyond the noise in the measurement at each corresponding temperature.

We characterized the apparent height of the TMV virus versus annealing time at the five temperatures studied. As shown in S7, at relative short time scales, the height of virus remains constant within the instrument error, and thus the surface diffusion mediates the surface flow at this short time window and results in meniscus formation as discussed in the main text. With the increase of annealing time and annealing temperatures, the virus starts to slowly embed into the film resulting in a decrease in apparent height. At this stage, the viscosity starts to drive the flow and the virus embeds into the film. The governing equation for embedding process is given by for surface viscosity control:

$$\frac{\partial h(x,t)}{\partial t} = -\frac{\gamma}{3\eta}\frac{\partial}{\partial x}[h^3(x,t)\frac{\partial^3 h(x,t)}{\partial x^3}] \tag{1}$$

or for bulk viscosity control:

$$\frac{\partial h(x,t)}{\partial t} = \frac{1}{2}\frac{\gamma}{\eta}\frac{\partial h(x,t)}{\partial x} \tag{2}$$

Mullins model

Here we present a brief discussion about the relevant driving forces for meniscus formation based on the Mullins model[6]. The full Mullins model includes the bulk viscosity, evaporation-condensation, bulk diffusion and surface diffusion as follows.

$$\frac{\partial h(x,t)}{\partial t} = A\frac{\partial h(x,t)}{\partial x} + B\frac{\partial^2 h(x,t)}{\partial x^2} + C\frac{\partial^3 h(x,t)}{\partial x^3} + D\frac{\partial^4 h(x,t)}{\partial x^4} \tag{3}$$

Where $A = \frac{1}{2}\frac{\gamma}{\eta}, B = \frac{p_0\gamma\Omega^2}{(2\pi M)^{1/2}(kT)^{3/2}}, C = \frac{\rho_0 D_G\gamma\Omega^2}{kT} + \frac{D_v\gamma\Omega}{kT}, andD = \frac{D_s\gamma\Omega^2\nu}{kT}$

Here γ is the surface tension, η is bulk viscosity, p_0 is the equilibrium vapor pressure, Ω is the molecular volume, ρ_0 is the equilibrium vapor density, D_G is diffusion coefficient of evaporated molecules in inert atmosphere, D_v is the bulk diffusion coefficient, ν is the number of atoms per unit area, and D_s is the surface diffusion coefficient. In this study, since the vapor pressure of TPD is very low at room temperature, there is no evaporation-condensation occurring during the course of this study. As such the evaporation-condensation term is negligible. Furthermore, at low temperatures used in this study the bulk diffusion is extremely slow (at least 4 orders of magnitude close to $\mathrm{T_g}$, and decreasing rapidly with decreasing temperature). As such the bulk diffusion can also be assumed to be negligible. This was further confirmed by the grating decay studies where gratings of various sizes were used to verify the scaling factors for the important terms in the Mullins model[7–9]. This leaves the bulk viscosity and surface diffusion terms. The bulk viscosity becomes important at the onset of embedding. Before that, when the only important term in the model that governs the meniscus formation is the surface diffusion term. This is also confirmed in our studies with the fact that the profiles are self-similar with $h(x,t) = h(x/t^{1/4})$, which follows the scaling law for surface diffusion. This can only be true if all other terms are negligible and surface diffusion controls the flow. Bulk viscosity, evaporation-condensation, and bulk diffusion follow different power-law and do not have the self-similar nature of $h(x,t) = h(x/t^{1/4})$. In addition, one can estimate the relative contribution from each term by estimating the prefactors order of magnitude and would find the other terms are much smaller (<1% compared to surface diffusion term) and cannot contribute to such fast surface evolution and thus can be neglected. Similar discussions can also be found in grating decay measurements[7–9].

The approximation used by Mullins to obtain the linearized surface diffusion equation (Equation 1 in main text) is the small slope approximation. In our system, as can be seen in Figure 2, even for the earliest time point measured, the slope can be estimated from the height and the width of the profiles to be h (17 nm) / width (200 nm) = 0.085, which is much smaller than 1, fulfilling the small slope approximation. In addition, the self-similarity observed in the experimental data is a strong indication of the validity of the Mullins linearized model, which only the surface diffusion term present.

Temperature dependence of relevant parameters

The molecular volume of TPD, Ω, used in this study was estimated from the molecular weight and relative density at 295 K as $\Omega = MW/(\rho \mathrm{N_A})$. The change in relative density can be estimated from the thermal expansion coefficient measured from temperature ramp measurements by ellipsometry. As shown in Figure S2, the glassy thermal expansion coefficient of TPD can be fitted from the thickness change with temperature to be $2.1 * 10^{-4} K^{-1}$, in the temperature range performed in the experiment 296 K to 318 K, the change in relative density is therefore estimated to be $\sim 0.5\%$. Compared to a factor of 4 change in the value of the prefactor observed in Figure 3 of the main text, this can be considered a negligible density change. However, we note that this change is mainly the error in our estimation of volume based on density and the actual molecular volume is most likely constant in this modest temperature range.

Using the Eötvös rule[10], we can roughly estimate the temperature dependence of surface tension of TPD by $\frac{\partial \gamma}{\partial T} = \frac{-k}{V^{2/3}}$, where k is the Eötvös constant and has a value of 2.1×10^{-7} J/(K$\cdot$ mol$^{2/3}$), V is the molecular volume for TPD, which is calculated based on the molecular weight and relative density, to be 4.34×10^{-4} m^3/mol. Thus $\frac{\partial \gamma}{\partial T}$ is calculated to be -3.66×10^{-5} N/(m$\cdot$ K). Compared to the surface tension of TPD at 295 K, which is equal to $\gamma = 7.23 \times 10^{-2}$ N/m, the changes in γ are negligible in the temperature range of the experiments reported here.

Comparison with surface diffusion of other molecular glasses

In S8, we compare the surface diffusion coefficient of TPD measured from TMV method in this study with other organic molecules measured using surface grating decay methods[8]. The surface diffusion coefficient of TPD at T_g is about 6 orders of magnitude than the bulk diffusion coefficient and fits well with other organic molecules, indicating that the surface diffusion coefficient has a strong molecular weight dependence.

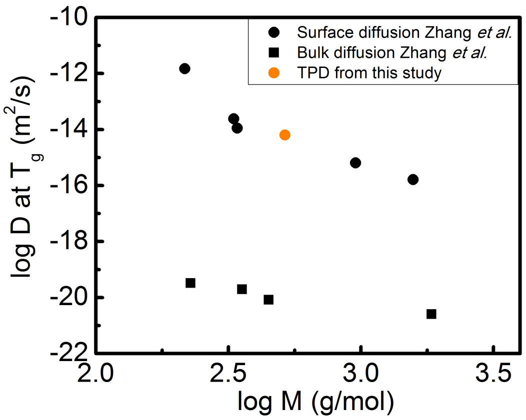

FIG. S8. Surface diffusion coefficient of TPD measured in this study extrapolated to T_g (orange circle) and other organic molecules (black circle) from the grating decay studies by Zhang *et al.*[8], and bulk diffusion coefficients (black square) at the material's bulk T_g.

[1] T. Liu, K. Cheng, E. Salami-Ranjbaran, F. Gao, C. Li, X. Tong, Y.-C. Lin, Y. Zhang, W. Zhang, L. Klinge, P. J. Walsh, and Z. Fakhraai, The Journal of Chemical Physics **143**, 084506 (2015).

[2] Y. Zhang, E. Glor, M. Li, T. Liu, K. Wahid, W. Zhang, R. Riggleman, and Z. Fakhraai, Submitted (2016).

[3] M. Benzaquen, P. Fowler, L. Jubin, T. Salez, K. Dalnoki-Veress, and E. Raphaël, Soft Matter **10**, 8608 (2014).

[4] T. Salez, J. D. McGraw, S. L. Cormier, O. Bäumchen, K. Dalnoki-Veress, and E. Raphaël, Eur. Phys. J. E. Soft Matter **35**, 114 (2012).

[5] J. D. McGraw, T. Salez, O. Bäumchen, E. Raphaël, and K. Dalnoki-Veress, Phys. Rev. Lett. **109**, 128303 (2012).

[6] W. W. Mullins, J. Appl. Phys. **30**, 77 (1959).

[7] L. Zhu, C. W. Brian, S. F. Swallen, P. T. Straus, M. D. Ediger, and L. Yu, Phys. Rev. Lett. **106**, 1 (2011).

[8] W. Zhang and L. Yu, Macromolecules **49**, 731 (2016).

[9] S. Ruan, W. Zhang, Y. Sun, M. Ediger, and L. Yu, The Journal of Chemical Physics **145**, 064503 (2016).

[10] Eötvös, Annalen der Physik **27** (1886).